Supporting Information

Study on Acetylcholinesterase Inhibition Induced by Endogenous Neurotoxin with Enzyme-Semiconductor Photoelectrochemical System

Wei Zhu,[a] Ya-Rui An,[a] Xiao-Min Luo,[b] Fei Wang,[b] Jiao-Hong Zheng,[a] Lin-Lin Tang,[a] Qing-Jiang Wang,[a] Zhong-Hai Zhang,[a] Wen Zhang,*[,a] Li-Tong Jin*[,a]

[a] *Department of Chemistry, East China Normal University, 3663 Zhongshan Rd.(N), Shanghai 200062, P.R. China,*

[b] *Center for Drug Discovery and Design, State Key Laboratory of Drug Research, Shanghai Institute of Meteria Medica, Shanghai Institutes of Biological Sciences, Chinese Academy of Sciences, 555 Zu Chong Zhi Road, Zhangjiang Hi-Tech Park, Shanghai 201203, P. R. China*

* Correspondence to wzhang@chem.ecnu.edu.cn

Preparation of AChE-Au-TiO_2 nanotubes. The electrochemical anodic oxidation technique was used to fabricate the TiO_2 nanotubes. Prior to anodization, Ti sheets were mechanically polished with different abrasive papers and rinsed in an ultrasonic bath of cold distilled water for 10 min. Then the cleaned Ti sheets were soaked in a mixture of HF and HNO_3 acids for 1 min (the mixing ratio of HF: HNO_3: H_2O is 1: 4: 5 in volume). After rinsed with acetone and deionized water for 10 min, the Ti sheets were dried in air at room temperature. The TiO_2 nanotubes were fabricated in a cylindrical electrochemical reactor (the radius is 30 mm and height is about 70 mm). 0.5 wt % hydrofluoric acid was used as the electrolyte and a platinum electrode served as the cathode during the entire process. A

potential of 20 V was used and anodization time of 20 min was spent in this experiment. Anodized Ti sheets were annealed in dry oxygen environment at 500 ℃ for 1 h; both heating and cooling rates were kept at 2.5 ℃ min^{-1}. Then, the well ordered and uniform TiO_2 nanotubes array was fabricated.

A novel photoelectrochemical deposition method was exploited to modify the resulting nanotubes with Au nanoparticles. The TiO_2 nanotubes served as the working electrode in a conventional photoelectrochemical cell, and a Ag/AgCl (3 M KCl) electrode and a platinum electrode served as the reference and counter electrode, respectively. The photoelectrochemical deposition of Au nanoparticles was carried out by cyclic voltammetry with the potential range from 0.0 to +1.4 V for 30 min under the irradiation of light at 253.7 nm wavelength. The photoelectroplating solution was prepared by dissolving 0.1 mM $HAuCl_4 \cdot 6H_2O$ in 0.5 M H_2SO_4 solution.

Then, 25 μL enzyme solution containing 1.0 mg/mL of acetylcholinesterase, 1.2 mg/mL of BSA and 2.5 % glutaraldehyde was dropped on one side of the Au-doped TiO_2 nanotubes and allowed to dry at room temperature. Before use the AChE-Au-TiO_2 nanotubes were rinsed with water to remove all physically absorbed materials.

Two methods for deposition of Au nanoparticles. The deposition of Au nanoparticles into TiO_2 nanotubes was carried out by conventional photodeposition technique and photoelectrochemical deposition method, respectively. In Figure S1a, Au nanoparticles produced by photodeposition method have been found to undergo some aggregation. On the contrary, photoelectrochemical deposition method leads to well-separated Au nanoparticles with a diameter in the range of 40 to 50 nm (Figure S1b). This may be due to the fact that the electric field in the TiO_2 nanotubes facilitates the plating solution to distribute well. Therefore, electrochemistry is likely to be of great importance in the formation of Au nanoparticles into TiO_2 nanotubes.

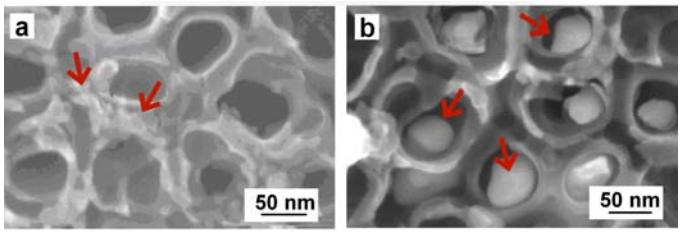

Figure S1. SEM images of Au-doped TiO_2 nanotubes prepared by (a) photodeposition method and (b) photoelectrochemical deposition method. Au nanoparticles are indicated by arrows.

EDX analysis of AChE-Au-TiO_2 nanotubes. Energy dispersive X-ray analysis (EDX) was used to characterize the Au-doped TiO_2 nanotubes. The EDX spectrum is presented in figure S2, which shows the strong diffraction peaks of elemental Ti at 4.51 and 4.92 KeV, the diffraction peak of elemental O at 0.52 KeV, and the diffraction peaks of Au at 1.70, 2.21 and 8.42. These results confirm that Au nanoparticles have been successfully deposited into TiO_2 nanotubes.

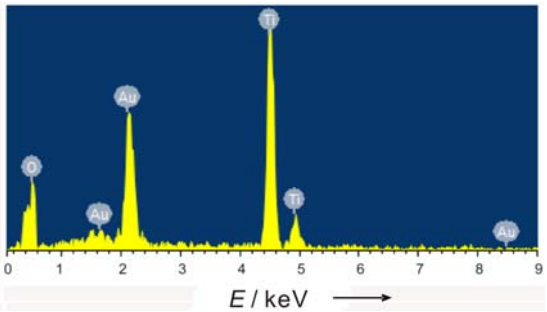

Figure S2. EDX spectra of Au-doped TiO_2 nanotubes.

Photocurrent responses in the presence of different ATCh concentrations. Figure S3 depicts the photocurrent responses of AChE-Au-TiO_2 hybrid system in the presence of different concentrations of ATCh. It is clear that with the increase of ATCh concentration, the photocurrent response is enhanced correspondingly. This is due to the fact that the hydrolysis of ATCh produces more thiocholine, which acts as a sacrificial electron donor to scavenge the holes. Hence, more electrons are accumulated in the conduction band of TiO_2 nanotubes, resulting in the increase of photocurrent. Moreover, the photoelectrochemical analysis has a low detection limit (50.0 pmol) for ATCh, which is attributed to the separation of excitation source and electrochemical detector.

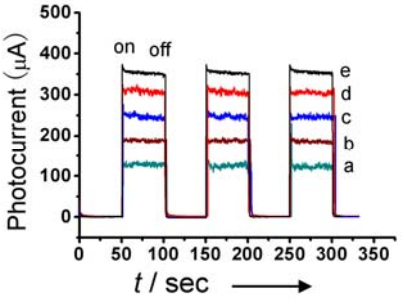

Figure S3. Photocurrent responses of AChE-Au-TiO_2 nanotubes hybrid system in the presence of different concentrations of ATCh, a) 20 μM, b) 40 μM, c) 60 μM, d) 80 μM, e) 100 μM. Data were recorded at a potential of 0.60 V in 0.10 M phosphate buffer (pH 7.4) under nitrogen; illumination with light of 253.7 nm.

Photocurrent responses of Au-TiO_2 nanotubes. As illustrated in Figure S4, Au-TiO_2 nanotubes yield the photocurrent responses under the illumination with light of 253.7 nm, which is attributed to the unique photoelectrochemical properties of TiO_2 nanotubes. However, the addition of ATCh into the Au-TiO_2 system doesn't produce effect on the photocurrent. The reason is that the hydrolysis of ATCh is halted due to the lack of AChE, and thereby the production of thiocholine, an electron donor, is inhibited.

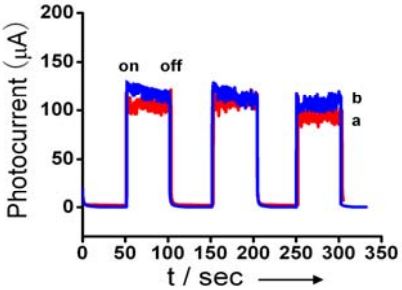

Figure S4. Photocurrent responses of Au-TiO_2 nanotubes in the (a) absence and (b) presence of ATCh. Data were recorded at a potential of 0.60 V in 0.10 M phosphate buffer (pH 7.4) under nitrogen; illumination with light of 253.7 nm.

Effect of illumination intensity. The illumination intensity has been considered to exert an effect on the photocurrent. Figure S5 reveals the dependence of photocurrent generated in AChE-Au-TiO_2 hybrid system on the light intensity. It has been found that there is a linear relationship between the photocurrent and light intensity, which implies that the photogeneration of charge carriers is a monophotonic process. The quantitative measure of photoelectrochemical properties is the incident photon to current efficiency (IPCE).[1] It can be estimated by the following equation:

$$IPCE = (I_\lambda hc) / (W_\lambda \lambda e)$$

where I_λ is the photocurrent, h the Planck constant, c the speed of light, W_λ the intensity of the incident light, λ the illumination wavelength, and e the electric charge of an electron. The IPCE value of ATCh in AChE-Au-TiO_2 hybrid system was found to be 17.6 %.

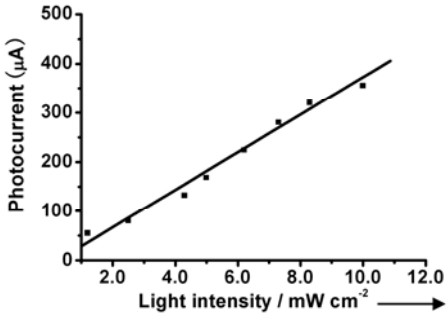

Figure S5. Dependence of photocurrent on the light intensity. Data were recorded at a potential of 0.60 V in 0.10 M phosphate buffer (pH 7.4) under nitrogen.

Effect of applied potential. The photocurrent-potential characteristics of AChE-Au-TiO_2 nanotubes were obtained in the absence and presence of ATCh. It can be seen from Figure S6 that with the increase of applied potential, the photocurrent is enhanced and gradually levels off at higher potential. This indicates that the photogenerated electrons in AChE-Au-TiO_2 system are effectively driven to the counter electrode by the positive potential, which can be beneficial to charge separation. In addition, the introduction of ATCh into the photoelectrochemical cell leads to a prominent enhancement in photocurrent with the potential ranging from -0.3 V to 0.9 V. This phenomenon can be explained by the generation of thiocholine, which is a product of AChE-catalyzed hydrolysis of ATCh and acts as a sacrificial electron donor. The presence of thiocholine provides a facile pathway for the transfer of holes, resulting in the higher photocurrent.

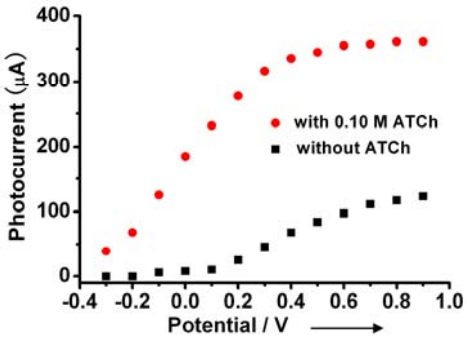

Figure S6. Dependence of photocurrent on the applied potential. Data were recorded in 0.10 M phosphate buffer (pH 7.4) under nitrogen; illumination with light of 253.7 nm.

Docking simulation. In order to give a clear picture about the interaction between (R)-NMSal and AChE, molecular docking simulation was carried out in this work. It can be seen from Figure S7 that both hydroxyl groups of (R)-NMSal are engaged in hydrogen bond formation with Tyr 155, Ser 147 and Trp 108 in AChE. Also, the hydrophobic interactions occur primarily between methyl of (R)-NMSal and hydrophobic residues of the pocket including Gly 143, Gly 495, Tyr 355, Gly 142, and His 494. Of great importance is that (R)-NMSal is likely to be bound near the bottom of the narrow gorge of AChE, a binding model resembling Huperzine (HupA) much (Figure S8).[2]

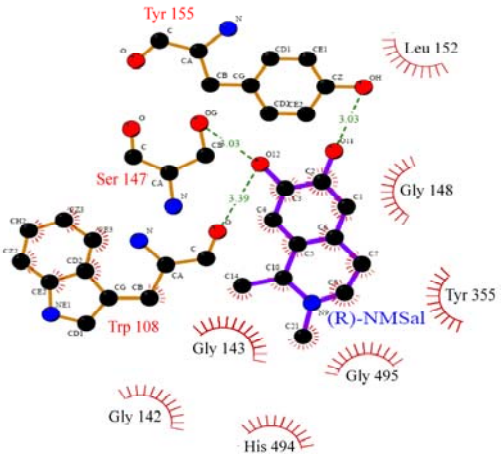

Figure S7. Schematic representation for the interaction mode of (R)-NMSal with AChE. Dashed lines represent hydrogen bonds and spiked residues form hydrophobic interactions with (R)-NMSal. This picture was made with the program LIGPLOT.[3]

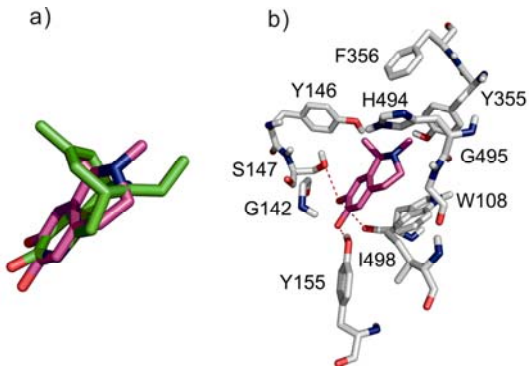

Figure S8. a) Comparison of docked (*R*)-NMSal (magenta) with HupA (green) bound in crystal structure. b) The proposed binding mode of (*R*)-NMSal (magenta) at the AChE gorge. The H-bonds are shown as dark-red dotted line. Only the amino acids close to the binding site are displayed.

Effect of HupA on the photocurrent responses. Figure S9 shows the influence of HupA on the photocurrent response generated in the AChE-Au-TiO_2 nanotubes hybrid system. It is evident that with the addition of 70.0 nM HupA, the photocurrent response decreases remarkably (Figure S9A, curve b). However, after the removal of HupA from the photoelectrochemical cell, the initial photocurrent is almost restored in the presence of 0.10 mM ATCh (Figure S9A, curve c). In addition, the Lineweaver-Burk analysis (Figure S9B) reveals that HupA exhibits a mixed inhibition against AChE, which is consistent with that previously reported. Based on these observations, we can conclude that this

semiconductor-enzyme hybrid system is of practical use for photoelectrochemical detection of the inactivation of AChE induced by inhibitors.

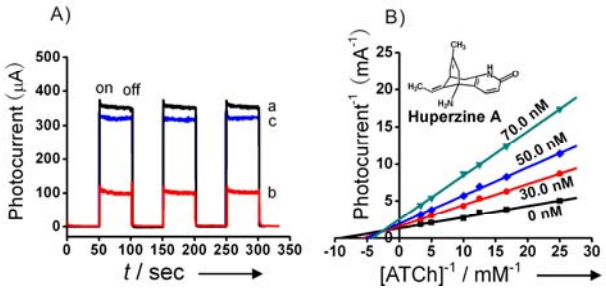

Figure S9. A) Photocurrent responses of AChE-Au-TiO_2 nanotubes hybrid system in the presence of 0.10 mM ATCh, a) without the inhibitor, b) with the addition of 70.0 nM HupA, c) after exclusion of the inhibitor. B) Lineweaver-Burke plots corresponding to the photocurrent of AChE-Au-TiO_2 nanotubes at variable concentrations of ATCh in the presence of different concentrations of HupA. Data were recorded at a potential of 0.6 V in 0.1 M phosphate buffer (pH 7.4) under nitrogen; illumination with light of 253.7 nm.

References

[1] L.A. Lyon and J.T. Hupp, *J. Phys. Chem.*, 1999, **103**, 4623.

[2] H. Dvir, H. L. Jiang, D. M. Wong, M. Harel, M. Chetrit, X. C. He, G. Y. Jin, G. L. Yu, X. C. Tang, I. Silman, D. L. Bai and J. L. Sussman, *Biochemistry*, 2002, **41**, 10810.

[3] A. C. Wallace, R. A. Laskowski and J. M. Thornton, *Protein Eng,*. 1995, **8**, 127.